Electrochimica Acta 102 (2013) 351–357

Contents lists available at SciVerse ScienceDirect

Electrochimica Acta

journal homepage: www.elsevier.com/locate/electacta

Characterization of niobium and vanadium oxide nanocomposites with improved rate performance and cycling stability

Ge Li [a,b], Xiaolei Wang [b], Zheng Chen [b], Xueming Ma [a,*], Yunfeng Lu [b,**]

[a] Department of Physics, East China Normal University, Shanghai 200241, China
[b] Department of Chemical and Biomolecular Engineering, University of California, Los Angeles, CA 90034, USA

ARTICLE INFO

Article history:
Received 20 February 2013
Received in revised form 23 March 2013
Accepted 25 March 2013
Available online 8 April 2013

Keywords:
Lithium-ion battery
High-performance anode
Niobium oxide
Nanocomposites
Synergistic effect

ABSTRACT

Niobium and vanadium oxides nanocomposites are synthesized using a facile sol–gel process, and characterized by scanning and transmission electron microscopy. X-ray diffraction results show that the nanocomposites are composed of Nb_2O_5 and its solid solutions. Such nanocomposites exhibit both significantly improved rate and cycling stability. At a current density of 1 A g^{-1}, the nanocomposites deliver more than three times of capacity than pure Nb_2O_5, and remain ~95% of its initial capacity after 50 cycles. Possible synergistic mechanism between the constituent components of the nanocomposites is also proposed.

1. Introduction

Lithium-ion batteries are essential power devices for portable systems, automotive applications and renewable energy storage [1–3]. Most commercial lithium-ion batteries utilize graphite as the anode with relatively high capacity (~372 mA h g^{-1}) and long cycling life [4]. However, its relatively low lithium-intercalation potential (~0.2 V versus Li/Li^+) may lead to lithium plating and dendrite growth, which brings significant safety concerns [5]. Moreover, carbon materials often exhibit low volumetric energy density resulted from low packing density [6]. By comparison, transition-metal oxides, such as lithium titanate ($Li_4Ti_5O_{12}$) [7,8] and titanium oxide (TiO_2) [9], possess higher lithium-intercalation potentials and packing densities, which are of great interest of lithium-ion battery applications. Niobium pentoxide (Nb_2O_5), in particular, has a comparable working potential (~1.5 V vs. Li^+/Li) to titanium-based oxides and reasonable specific capacity (~201 mA h g^{-1}) [10–12], which makes it a highly promising material candidate. The implementation of Nb_2O_5-based electrode, however, has been intrinsically limited by its poor electric conductivity ($\sigma \sim 3 \times 10^{-6}$ S cm^{-1}) [13] and slow ion diffusion, which results in low rate performance. Moreover, the capacity decay caused by volume expansion [14] during lithiation also brings certain concerns on its cycle life in practical application.

To date, several methods have been explored to improve the rate capability of Nb_2O_5, most of which mainly focus on forming effective path for ion migration or building network for electron transportation [15,16]. The first approach involves the formation of mesoporous Nb_2O_5 thin film on conductive substrates [17]. Compared with the bulk counterpart, such a thin film reduces the resistance for both electron and ion transport, leading to an outstanding rate performance. However, low mass loading of the active material results in low energy density. The second approach relies on combining Nb_2O_5 nanoparticles with conductive agents (e.g. carbon black [10] and carbon nanotubes [18]). Although the conductive agents form a continuous conductive network while the nanoparticles shorten the ion-diffusion pathway, the Nb_2O_5/carbon interface may be destructed easily during charge–discharge process, which results in poor cycling life. On the other hand, it has also been reported that doping Nb_2O_5 with other elements or forming Nb_2O_5-based solid solutions can improve either the rate capability or the cyclability of Nb_2O_5 [19,20]. Compared with pure Nb_2O_5, the introduction of foreign atoms changes the local structure and electronic property around Nb atoms [21]. For example, the conductivity of Cs-doped Nb_2O_5 [22] can be increased to 10^{-5} S cm^{-1}, while Ta-doped Nb_2O_5 [20] shows a superior stability. Recently, Goodenough group utilized $TiNb_2O_7$ solid solution with much higher reversible specific capacity (~285 mA h g^{-1}) as anode material [12,23]. The rate performance, however, is still not satisfactory unless extra carbon coating is adopted.

Herein, we report a synthesis of Nb_2O_5-based nanocomposites with significantly improved rate performance and cycling

* Corresponding author. Tel.: +86 21 5434 2731.
** Corresponding author. Tel.: +1 310 794 7238; fax: +1 310 206 4107.
E-mail addresses: xmma@ecnu.edu.cn (X. Ma), luucla@ucla.edu (Y. Lu).

0013-4686/$ – see front matter © 2013 Elsevier Ltd. All rights reserved.
http://dx.doi.org/10.1016/j.electacta.2013.03.169

stability using a facile sol–gel process. By introducing vanadium (V) into Nb_2O_5, the rate performance was greatly improved. Furthermore, such composite electrodes show enhanced cycling stability, which cannot be reached in Nb-doped V_2O_5 composites [24]. Possible synergistic mechanism between the constituent components of the nanocomposites that leads to such rate and cyclic stability were also proposed. This work provides a new material design concept toward better electrode materials with improved energy and power density.

2. Experimental

Synthesis and characterization of Nb_2O_5 nanocomposites. A simple sol–gel technique was applied to synthesize the Nb_2O_5-based nanocomposites. In a typical synthesis, ammonium niobate (V) oxalate hydrate (3.26 mmol, 0.989 g) and ammonium metavanadate (0.52 mmol, 0.610 g) were dissolved in DI-water (30 mL) under ultrasonication for 30 min, followed by adding HCl solution (2.0 M, 0.5 mL) under stirring. The clear and transparent solution was transferred to a petri-dish and kept overnight at room temperature to allow the evaporation of the solvent. The colorless gel was then sintered at 550 °C in air for 5 h with a ramp rate of 1 °C min^{-1} from room temperature to 350 °C, and 5 °C min^{-1} from 350 to 550 °C. The product was then collected and denoted as VNb-*X*, where *X* corresponds to the weight percentage of V_2O_5 in the whole composite. The pure V_2O_5 and Nb_2O_5, and composites with different ratios were also synthesized following the same procedure. The color of the composites is from white to yellow-brown with increasing the V_2O_5 content.

X-ray diffraction (XRD) experiments were conducted on a X'Pert Pro X-ray diffractometer (Panalytical B.V.); scanning electron microscopic (SEM) experiments were conducted on a JEOL JSM-6700 FE-SEM (JEOL); transmission electron microscopic (TEM) experiments were conducted on a Philips CM120 operated at 120 kV (Philips/FEI).

Electrode fabrication and characterization. A certain amount of the composite was dispersed in *N*-methylpyrrolidinone (NMP) by ultrasonication and stirring to form homogeneous and stable slurries, where 10 wt% poly(vinylidene fluoride) (PVDF) and 10 wt% carbon black were also added. The composites electrodes were prepared by coating the slurries onto nickel foil current collector and dried at 100 °C overnight. The mass loading was controlled to be ~5 mg cm^{-2} on each current collector.

Cyclic voltammetry measurements were carried out on a VMP3 potentiostat/galvanostat (Bio-Logic LLC, Knoxville, TN). $LiClO_4$ in propylene carbonate (PC) (1 M) was used as the electrolyte, and lithium foils were used as both the counter and reference electrodes. Cyclic voltammetric (CV) measurements were carried out in an argon-filled glove box using cutoff voltages of 3.0 and 1.0 V versus Li^+/Li at different scan rates. The charge and discharge measurements were carried out on standard 2032-type coin cells by LAND CT2000 (Wuhan Jinnuo Electronics, Ltd., Wuhan, China) at different current densities. The cells were assembled in a glovebox under an argon atmosphere, where 1 M $LiPF_6$ in EC/DMC (1:1) was used as the electrolyte. Electrochemical impedance spectroscopy (EIS) tests were carried out on a Solartron 1860/1287 Electrochemical Interface.

3. Results and discussion

Fig. 1 shows the X-ray diffraction (XRD) patterns of as-synthesized Nb_2O_5, V_2O_5, and Nb_2O_5-based composites. The pure Nb_2O_5 (Fig. 1, bottom curve) exhibits a highly crystalline structure (pseudo-hexagonal structure, JCPDS No. 07-0061) [25], while the patterns of the V_2O_5 (Fig. 1, top curve) could be indexed to

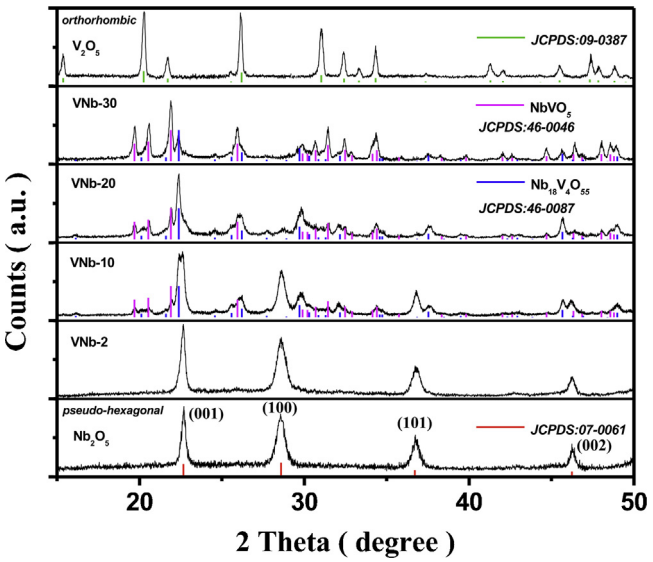

Fig. 1. XRD patterns of as-synthesized Nb_2O_5, V_2O_5, and nanocomposites with different V compositions.

an orthorhombic phase (JCPDS No. 09-0387). The diffraction patterns of the VNb composites suggest that they are composed of Nb_2O_5 and solid solutions of $NbVO_5$ (orthorhombic structure, JCPDS No. 46-0046) and $Nb_{18}V_4O_{55}$ (orthorhombic structure, JCPDS No. 46-0087) (see Fig. S1 in supporting information), with no obvious indications of V_2O_5 or other impurities. More specifically, Nb_2O_5 is the dominant phase in VNb-2 and VNb-10. The content of the solid solutions increases with increasing V content, accompanying by decreasing Nb_2O_5 content. For VNb-30, nearly all of the Nb_2O_5 is present in the form of solid solutions. Moreover, a slight shift of (0 0 1) peak from Nb_2O_5 can be observed with increasing V content, indicating an increase in lattice spacing.

The morphology of the composites was characterized by SEM (see Figs. 2 and S2). Fig. 2 shows the representative low and high magnification SEM images of the pure Nb_2O_5, pure V_2O_5 and VNb-10. Homogeneous particle morphology can be observed for the pure Nb_2O_5 (Fig. 2(a) and (b)) with particles size varying around tens of nanometers with agglomeration. The V_2O_5 are found to be bar-like crystals of submicron size (Fig. 2(e) and (f)). Particulate morphology with agglomeration is maintained for composite VNb-10, as shown in Fig. 2(c) and (d). The particle sizes fall between Nb_2O_5 and V_2O_5, implying the interactively restraining during the formation of nanocomposite. This size-increase trend is also found in all composites (see Fig. S2), as increasing the vanadium composition, reflecting the increase in crystallinity, which is confirmed by XRD results. TEM images also confirm the shape and size of the crystals. As shown in Fig. 3, the Nb_2O_5 particles have an average size of around 40 nm with agglomeration; the V_2O_5 bars are 300–400 nm in diameter and around 1 μm in length. The high-resolution images show high crystalline feature of the pure compounds, as well as the composites (Figs. 3(c) and (d) and S3).

Electrochemical behavior of the samples was examined using cyclic voltammetric (CV) measurements. Generally, electrochemical Li^+ insertion in Nb_2O_5 can be described by $Nb_2O_5 + xLi^+ + xe^- \leftrightarrow Li_xNb_2O_5$ [14,26,27]. Fig. 4 compares the first- and second-cycle CV curves of Nb_2O_5, V_2O_5 and VNb-10 normalized with respect to the active mass using a sweeping rate of 0.2 mV s^{-1} at room temperature. The Nb_2O_5 shows two distinct anodic peaks located at potential of 1.75 and 1.45 V, where the reduction of Nb_2O_5 from Nb^{5+} to Nb^{4+} by two Li^+ ions occurs at two lithium-intercalation sites with different reaction energies. In contrast, a broad cathodic peak can be observed in the Li^+ de-intercalation